Design and Analysis of EBG Based Integrated Waveguide Structures for Microwave and MM-Wave Feed Networks





T.J. Coenen^(1,2), A. Mazzinghi^(1,3), D.J. Bekers⁽¹⁾, A. Neto⁽¹⁾, J.L. Tauritz⁽²⁾, A. Freni⁽³⁾, G. Gerini⁽¹⁾

- (1) TNO Defence, Security and Safety, The Hague, The Netherlands
 - (2) University of Twente, Enschede, The Netherlands
 - (3) University of Florence, Florence, Italy

teis.coenen@tno.nl

Abstract

Traditional planar transmission lines (e.g. microstrip lines) require thinner substrates at higher frequencies, resulting in narrow metal strips. Consequently the electric current is confined to a smaller volume and losses increase in these structures.

Wave-guiding structures that are based on parallel plate waveguides with periodic side walls constructed of either metallic or dielectric posts can enlarge the current carrying volume and thus reduce losses.

Using an element-by-element method we demonstrate that in dielectric post-wall waveguides the propagation of the TE_{10} mode is dominant just as in metallic post-wall waveguides. The losses in both types of waveguides are of comparable order if a proper geometry is chosen.

1. Post-wall waveguides

The post-wall waveguide consists of two parallel metal plates which are latterly bounded by arrays of pins (see Figure 1).

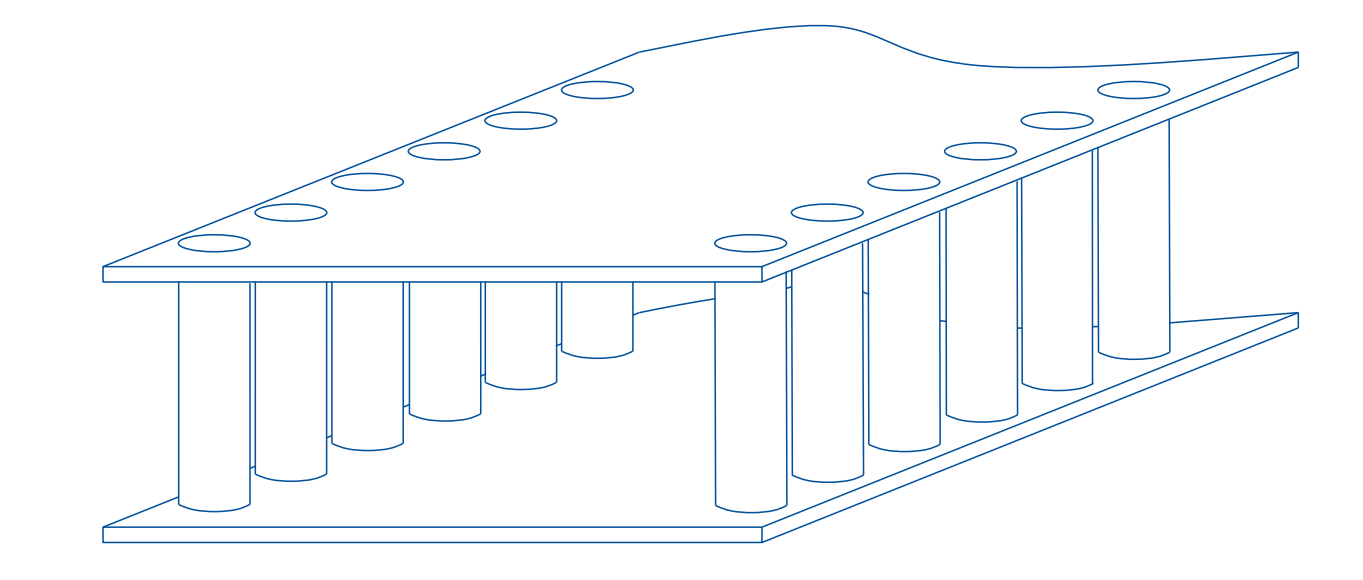


Figure 1: impression of a post-wall waveguide

The arrays of pins act as a reflecting surface, equivalent to the walls of a rectangular waveguide. The pins can be either *metallic* or *dielectric*.

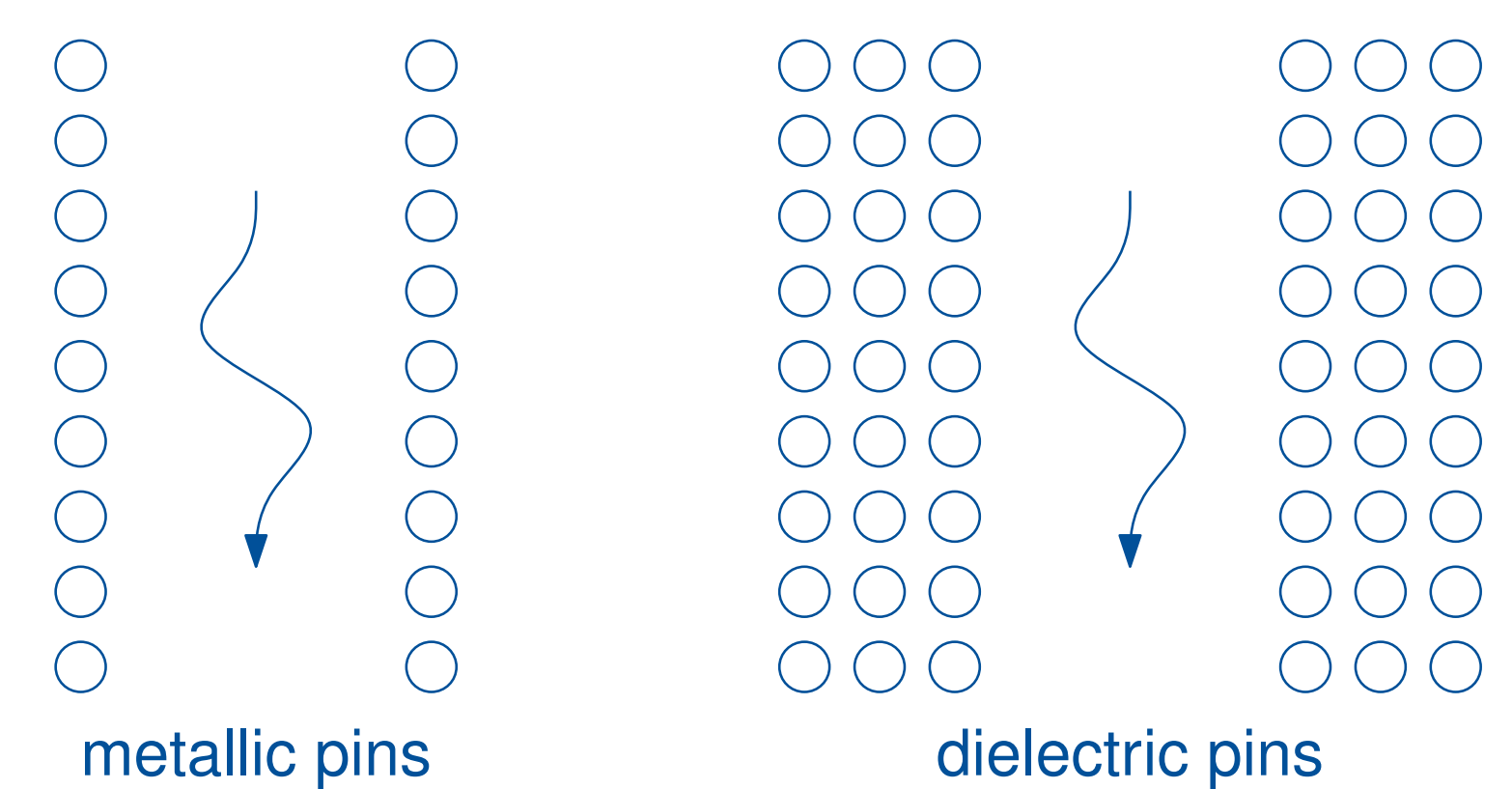


Figure 2: top view of post-wall waveguides

Metallic pins are good reflectors; an array consisting of a single row of pins is sufficient as reflecting wall.

Dielectric pins reflect less; arrays consisting of multiple rows, acting as an EBG, are necessary to obtain a reflecting wall.

2. Analysis

The dominant mode of propagation in post-wall wave-guides is a perturbed variant of the TE_{10} mode of classic rectangular waveguides. For metallic post-wall waveguides this is plausible, but it is not obvious for dielectric post-wall waveguides.

The distance between the effective reflection planes of the post-wall waveguide, $w_{g,eff}$, equals the width of the rectangular waveguide. This distance depends on the geometry and is related to the propagation angle ϕ_i by

$$\phi_i = \arcsin \frac{\lambda}{2 w_{\pi, off}} \tag{1}$$

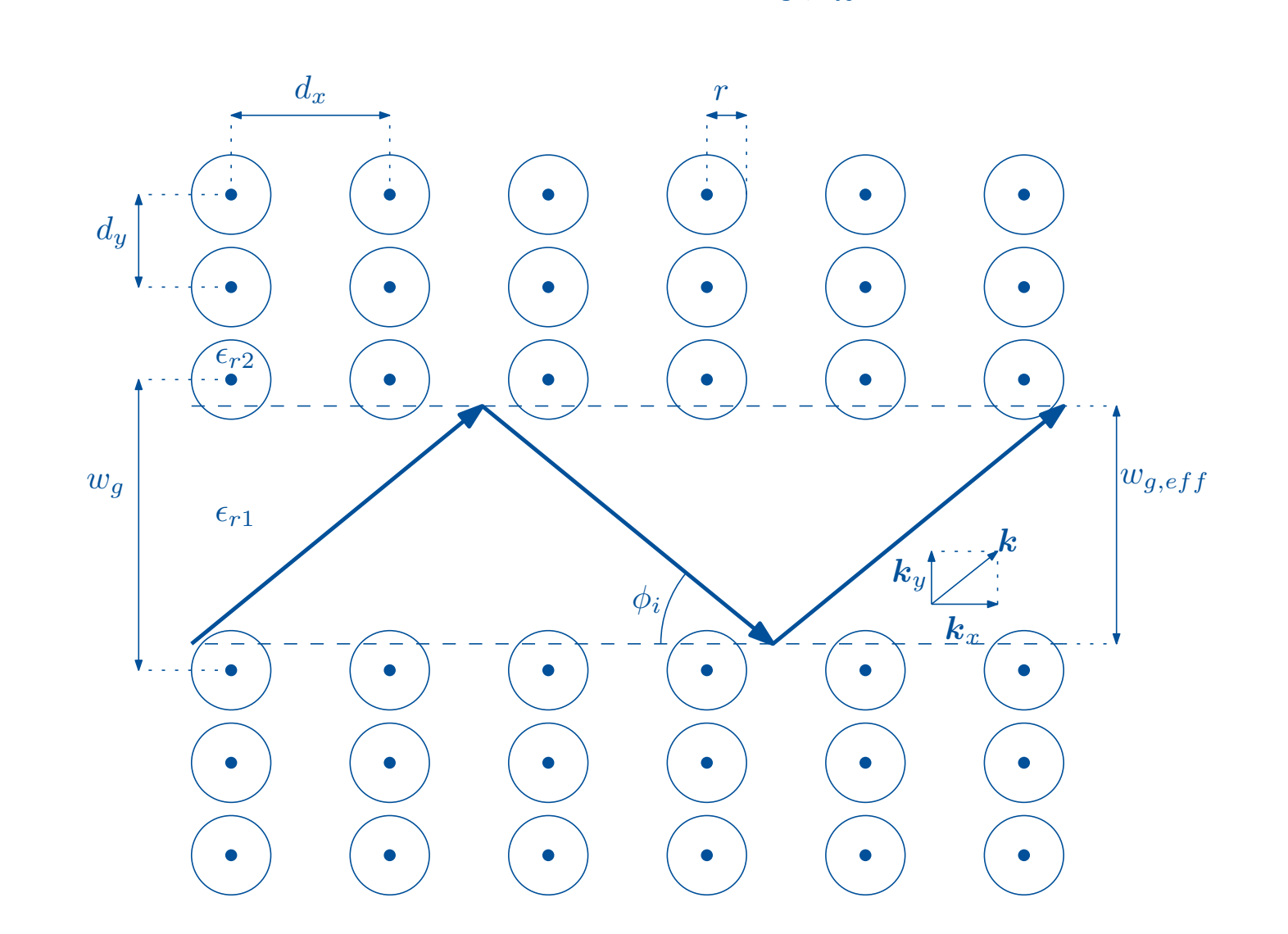


Figure 3: geometry of the post-wall waveguide

We use an element-by-element method to determine the waveguide characteristics required for wave propagation. In the simplest form we only consider the dominant spectral mode by looking at the plane-wave reflection at a single side wall. A more accurate approach analyzes the plane-wave propagation between the two side walls of the post-wall waveguides, thereby considering the coupling between the side walls.

Approach 1 (simplified approach) fixes the angle of incidence ϕ_i and observes the spatial position of the second null in the standing wave pattern to determine w_q .

Approach 2 (full interaction) consists the following: an initial w_g is chosen, next the angle of incidence ϕ_i is determined at which a wave with a perpendicular equiphase front is propagating and finally if ϕ_i is not the desired angle a new w_g is chosen and the cycle is repeated.

3. General electromagnetic model

In our analytical model for post-wall waveguides with metallic or dielectric pins we assume that

- 1. the cylinders are homogeneous,
- 2. the cylinders extend infinitely in the axial direction, and3. only an electric field in the axial direction exists.

These assumptions reduce the 3D problem to a 2D problem:

$$\boldsymbol{E} = E_z \boldsymbol{i}_z \tag{2}$$

An incident electric field ${m E}^i$ induces electric currents ${m J}$ in the cylinders. These currents give rise to a scattered electric field

$$\boldsymbol{E}^{s}(\boldsymbol{x}) = \int \boldsymbol{G}^{e}(\boldsymbol{x}; \boldsymbol{x'}) \boldsymbol{J}(\boldsymbol{x'}) d\boldsymbol{x'}$$
 (3)

4. Metallic pins

The boundary condition at the surface of the cylinders implies that the tangential electric field vanishes:

$$E_z^s = -E_z^i \tag{4}$$

The combination of equations 3 and 4, and the projection of the currents and the incident electric field on basis and test functions leads to a matrix equation

$$[\boldsymbol{Z}][\boldsymbol{I}] = [\boldsymbol{E}^i] \tag{5}$$

We use Galerkin's method and we define the expansion functions at the circumference of each cylinder n as

$$f_n^{(b)}(\phi_n) = \frac{1}{2\pi r} e^{-jb(\phi_n - \phi_i)}$$
 (6)

In matrix equation 5, the coupling matrix [Z] is a block matrix of $M \times N$ blocks of $T \times B$ matrices, whose elements are

$$Z_{mn,tb} = -\frac{k\zeta}{4} \begin{cases} 0 & (m = n, b \neq -t) \\ J_b(kr)H_b^{(2)}(kr) & (m = n, b = -t) \\ J_b(kr)J_{-(b+t)}(kr) & \times H_{-t}^{(2)}(k(m-n)d_x) & (m \neq n) \end{cases}$$
(7)

5. Dielectric pins

The surface of the cylinders ensures that the total tangential electric field is continuous across the cylinder boundary:

$$E_{z,1}^s + E_{z,1}^i = E_{z,2}^s + E_{z,2}^i \tag{8}$$

The field can be represented by an equivalent current at the cylinder boundaries

$$J_z = j\omega(\epsilon_2 - \epsilon_1)(E_z^s + E_z^i)$$
(9)

We combine equations 3, 8 and 9 and write the Method of Moments matrix equation as the relation between the total electric field and the incident electric field at the cylinder boundary

$$[C][E] = [E^i] \tag{10}$$

For cylinders small compared to the wavelength we describe the electric field in the cylinders by a constant function and we test the incident field at the center of each cylinder. The elements of the coupling matrix are

$$C_{mn} = \begin{cases} 1 + \frac{j}{2}(\epsilon_2 - \epsilon_1)[\pi k_1 r H_1^{(2)}(k_1 r) - 2j] & (m = n) \\ \frac{j\pi k_1 r}{2}(\epsilon_2 - \epsilon_1)J_1(k_1 r) H_0^{(2)}(k_1 \rho_{mn}) & (m \neq n) \end{cases}$$
(11)

6. Results

We first consider the metallic post-wall waveguide and we use the method of Section 4 to compute the total electric field. In our computations we use the following parameters:

$$\epsilon_{r1}$$
 = 10
 $w_{g,eff}$ = 0.85 λ_1
 r = 0.0667 λ_1
cyl. in x -dir. = 100 per side wall

We excite the TE_{10} mode in the waveguide. Figure 4a and b show the strength and the phase of the electric field in the (x,y)-plane.

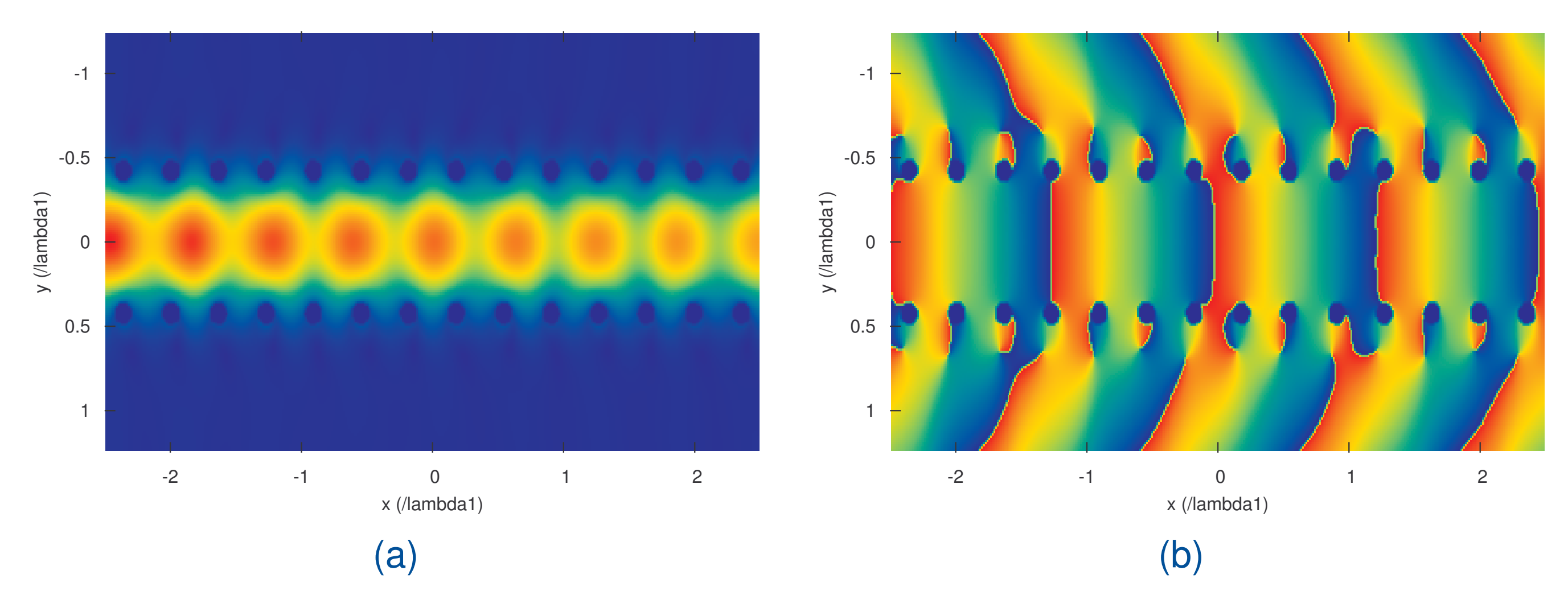


Figure 4: amplitude (a) and phase (b) of the electric field in the (x, y)-plane in a metallic post-wall waveguide

Figure 5 shows the relation between the waveguide width w_g and the pin spacing in the direction of the x-axis d_x at a fixed frequency and for a fixed effective waveguide width $w_{g,eff}$. Figure 5a shows the results for approach 1 (single side wall) and Figure 5b shows results for approach 2 (two side walls). Both results are plotted for 1, 3, 5 and 7 expansion functions per cylinder and a result from the literature (Figure 5 in [1]) is plotted as well.

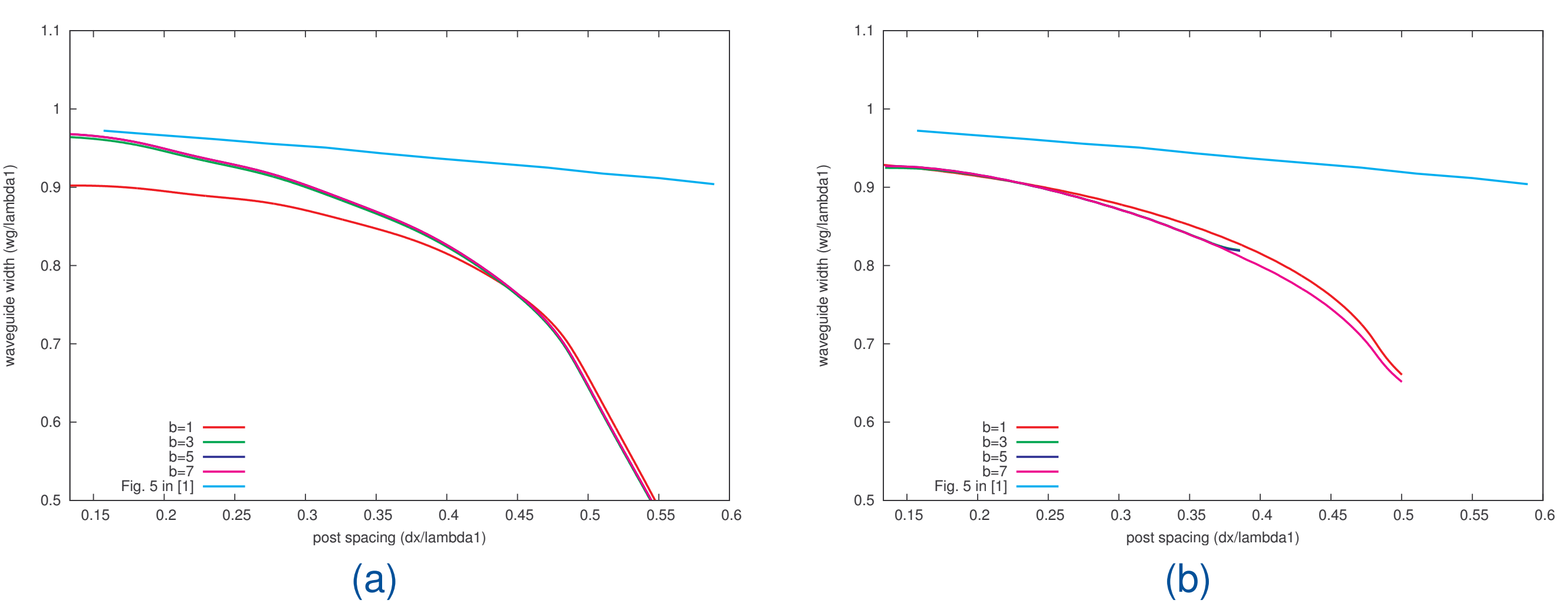


Figure 5: w_g as a function of d_x with (a) and without (b) higher order coupling in a metallic post-wall waveguide

The normalized dispersion curve for a metallic post-wall waveguide with post spacing in the x-direction $d_x = 0.2\lambda_1$, as well as the dispersion curve of a solid-wall rectangular waveguide are plotted in Figure 6.

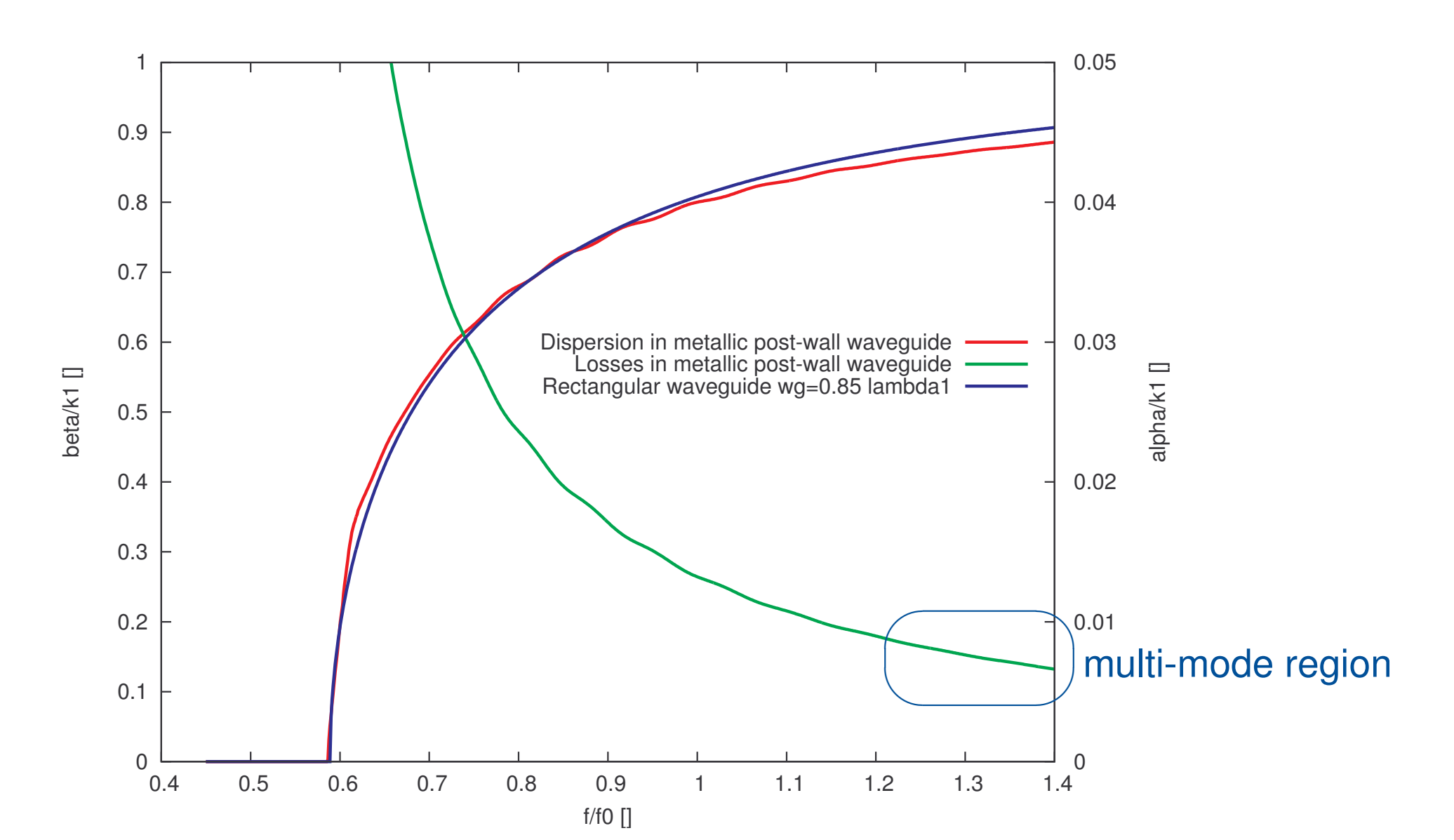


Figure 6: normalized dispersion curve of the TE_{10} mode in a metallic post-wall waveguide

In the case of the dielectric post-wall waveguide we use the parameters as specified bellow.

$$\begin{array}{ll} \epsilon_{r1} &= 10 \\ \epsilon_{r2} &= 1 \\ w_{g,eff} &= 0.85 \quad \lambda_1 \\ r &= 0.0667 \quad \lambda_1 \\ dy &= 0.25 \quad \lambda_1 \\ \text{cyl. in } x\text{-dir.} = 100 \quad \text{ per side wall} \\ \text{cyl. in } y\text{-dir.} = 3 \quad \text{ per side wall} \end{array}$$

The excitation of the TE_{10} mode leads to the electric field plots of Figure 7a and b for amplitude and phase in the (x,y)-plane.

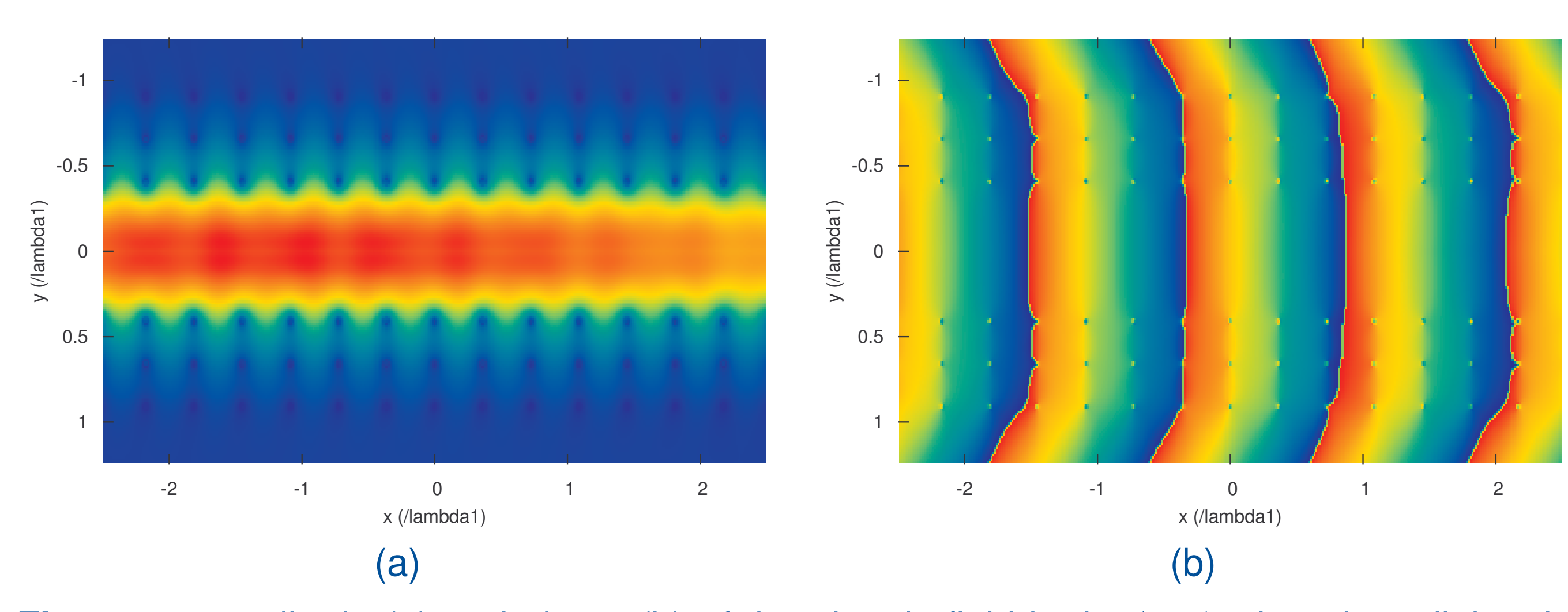


Figure 7: amplitude (a) and phase (b) of the electric field in the (x, y)-plane in a dielectric post-wall waveguide

Figures 8a and b show the relation between pin-spacing along the x-axis and the required width of the waveguide at the fixed effective width.

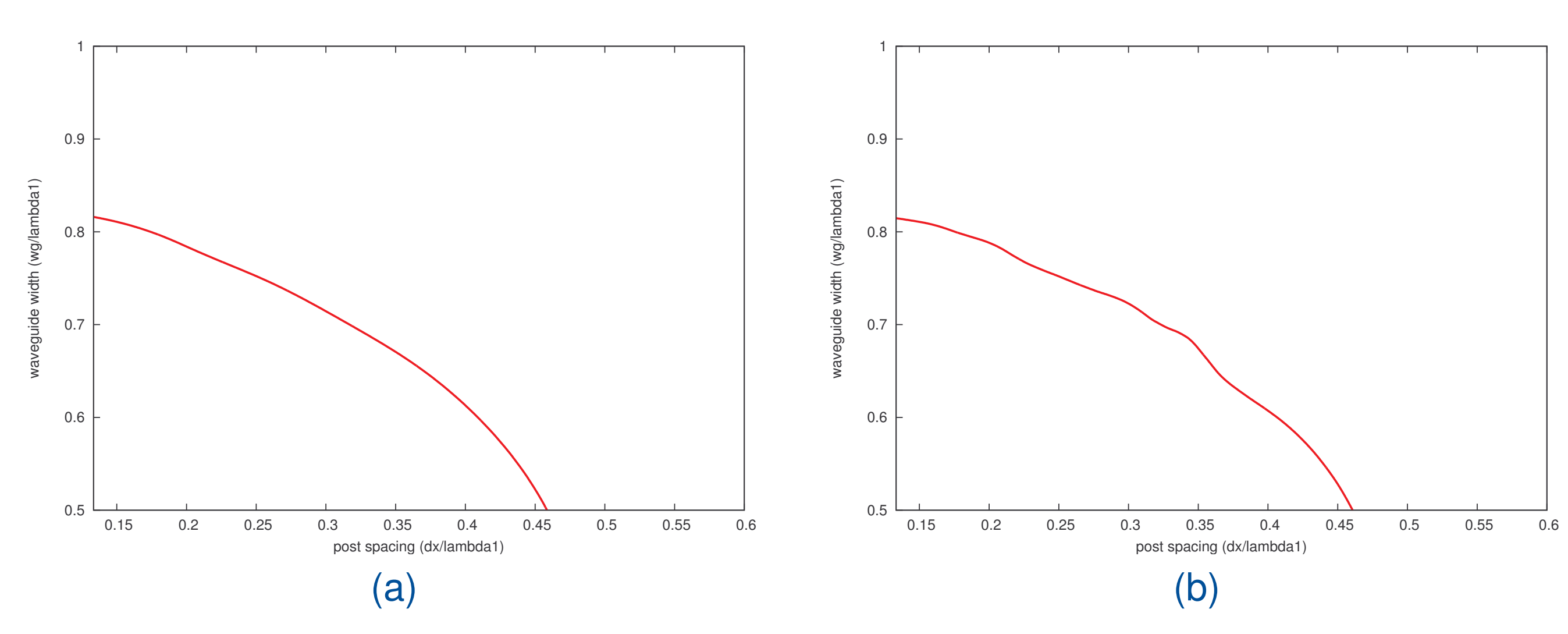


Figure 8: w_g as a function of d_x with (a) and without (b) higher order coupling in a dielectric post-wall waveguide

The dispersion curve for the dielectric post-wall waveguide ($d_x = 0.2\lambda_1$) is plotted in Figure 9, together with the curves of solid-wall metallic rectangular waveguides with $w_g = w_{g,eff}$ at $f = f_1$ ($w_g = 0.85\lambda_1$) and $f = f_{cutoff}$ ($w_g = 1.07\lambda_1$).

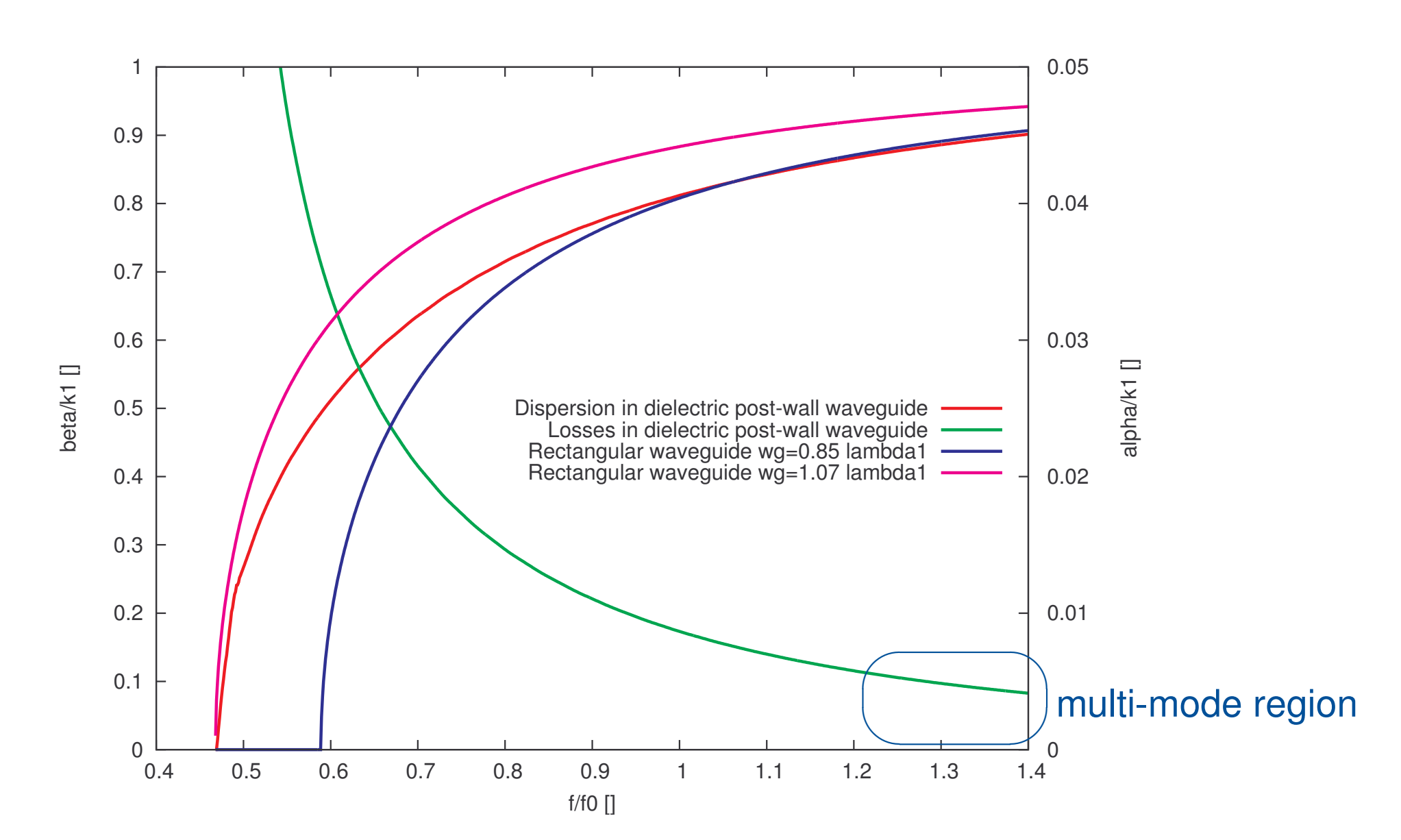


Figure 9: normalized dispersion curve of the TE_{10} mode in a dielectric post-wall waveguide

We note that

- ripples on the curves that are caused by the finiteness of the waveguide are smoothed by a regression algorithm, and
- ullet at $d_x=0.62\lambda_1$ the first grating lobe is launched, which causes the steep decrease of the w_g , d_x curves in Figures 5 and 8.

7. Discussion

In Figure 6 the propagation of the TE_{10} mode in a metallic post-wall waveguide is shown to be quite similar to the propagation of that mode in a rectangular waveguide. From Figure 5 we see that our results differ considerably from previous work performed by Hirokawa and Ando [1], however, our results show excellent agreement with recent work by Deslandes and Wu [2].

The dispersion characteristics of the dielectric post-wall waveguide, as depicted in Figure 9, show that this guide has a less dispersive behavior, resulting in a lower cutoff frequency. The losses in both types of waveguide are of comparable order, but the dielectric post-wall waveguide shows a much flatter curve. Analysis of waveguides with periodic dielectric slab-walls and simulations with commercial software tools indicate that the use of larger dielectric cylinders can further reduce the losses in this type of waveguide.

8. Conclusions

We designed a dielectric post-wall waveguide and we demonstrated that the dominant propagating mode is the TE_{10} mode, as in a metallic post-wall waveguide. In both structures the losses due to leakage are low and of comparable order.

9. Future work

In the future we will extend this work by

- improving the model to cope with larger dielectric cylinders,
- deriving design guidelines to optimize bandwidth versus losses and dimensions of dielectric post-wall waveguides,
- designing vertical transitions using rectangular slots in the metal planes and
- integrating post-wall waveguides with front-end electronics and antennas.

References

- [1] J. Hirokawa and M. Ando, "Single-layer feed waveguide consisting of posts for plane TEM wave excitation in parallel plates," *IEEE Transactions on Antennas and Propagation*, vol. 46, no. 5, pp. 625–630, May 1998.
- [2] D. Deslandes and K. Wu, "Accurate modelling, wave mechanisms, and design considerations of a substrate integrated waveguide," *IEEE Transactions on Microwave Theory and Techniques*, vol. 54, no. 6, pp. 2516–2526, June 2006.
- [3] J.H. Richmond, "Scattering by a dielectric cylinder of arbitrary cross section shape," *IEEE Transactions on Antennas and Propagation*, vol. 13, no. 3, pp. 334–341, May 1965.
- [4] R. Biswas I. El-Kady, M.M. Sigalas and K.M. Ho, "Dielectric waveguides in two-dimensional photonic bandgap materials," *IEEE/OSA Journal of Lightwave Technology*, vol. 17, no. 11, pp. 2042–2049, November 1999.